



OPEN

Relationship between intrathrombotic appearance of HSP27 and HSP70 and thrombus ages in a murine model of deep vein thrombosis

Mizuho Nosaka¹, Yuko Ishida¹, Yumi Kuninaka¹, Akiko Ishigami¹, Akira Taruya², Emi Shimada¹, Yumiko Hashizume¹, Hiroki Yamamoto¹, Akihiko Kimura¹, Fukumi Furukawa^{1,3} & Toshikazu Kondo¹✉

Heat shock proteins (HSPs) are molecular chaperones whose primary function is cytoprotection, supporting cell survival under (sub) lethal conditions. They have been implicated in various diseases such as inflammatory diseases and cancer due to their cytoprotective and immunomodulatory effects, and their biological mechanisms have been studied. Central family members include, HSP27, which is induced by various stimuli such as heat shock, hypoxia, hyperoxia, ultraviolet exposure, and nutritional deficiency, and HSP70, which is homeostatically expressed in many organs such as the gastrointestinal tract and has anti-cell death and anti-inflammatory effects. In this study, HSP27 and HSP70 were investigated during thrombus formation and dissolution in a deep vein thrombosis model by immunohistochemistry to determine their involvement in this process and whether their expression could be used as a forensic marker. In the process of thrombus formation and lysis, HSP27 and HSP70 were found to be expressed by immunohistochemical analysis. The role of inhibitors of HSP27 and HSP70 in the pathogenesis of thrombosis in mice was also investigated. When HSP27 or HSP70 inhibitors were administered, thrombi were significantly smaller than in the control group on day 5 after inferior vena cava ligation, indicating pro-thrombotic effects HSP27 and HSP70. If HSP27- or HSP70-positive cells were clearly visible and easily identifiable in the thrombus sections, the thrombus was presumed to be more than 10 days old. Thus, the detection of intrathrombotic HSP27 and HSP70 could forensically provide useful information for the estimation of thrombus ages. Collectively, our study implied that both HSP27 and HSP70 might be molecular targets for thrombus therapy and that the detection of HSP-related molecules such as HSP27 and HSP70 could be useful for the determination of thrombus ages.

Heat shock proteins (HSPs) are a family of proteins that are produced in cells by various stimuli, such as high temperature, hypoxia, hyperoxia, UV exposure, nutrient deprivation, and other stressors, and their main role is to maintain cellular homeostasis and to promote cell survival. HSP27 is known as the HSPB family that are ubiquitously present in mammalian cells and are encoded by the heat shock protein beta-1 (HSPB1) gene¹. HSP27 exhibits chaperone-like activity, prevents aggregation of partially unfolded proteins, protects cells from oxidative stress by scavenging reactive oxygen species (ROS), and protects cells from apoptosis in response to stress conditions by blocking cytochrome c and inhibiting caspase-3 activation^{2,3}. HSP70 is a member of the HSPA family, and it has been assumed to protect the cell via its chaperone functions. Indeed, overexpression of HSP70 appears to prevent protein aggregation and redistribution of ubiquitin⁴.

¹Department of Forensic Medicine, Wakayama Medical University, 811-1 Kimiidera, Wakayama 641-8509, Japan. ²Department of Cardiovascular Medicine, Wakayama Medical University, 811-1 Kimiidera, Wakayama 641-8509, Japan. ³Takatsuki Red Cross Hospital, 1-1-1 Abuno, Takatsuki, Osaka 569-1096, Japan. ✉email: kondot@wakayama-med.ac.jp

In this study, we aimed to establish a new index for determining the degree of thrombus obsolescence by immunohistochemically analyzing the dynamics of heat shock proteins over time in order to find the possibility that stress proteins are involved in the process of thrombus formation and dissolution^{5–9}.

From a forensic perspective, pulmonary thromboembolism resulting from deep vein thrombosis (DVT) is one of the leading causes of sudden unexpected death. We have elucidated the pathogenesis of DVT from both forensic and experimental pathology^{10,11}. Later, using knockout mice, we found that cytokines such as IFN- γ , TNF- α and IL-6 play an important role in the resolution of DVT^{12–14}. Determining the elapsed time taking for a wound to persist or for a thrombus to form is one of the important matters^{15–21}. Therefore, we reported several specific cells and markers for thrombus age estimation^{10,11}.

The HSP expression under heat stress has already been demonstrated in myocardium, lung and kidney tissues and HSPs can be visualized with immunohistochemical staining^{22–24}. Not only fire deaths but also cardiac deaths, mechanical asphyxiation and acute lung injury, HSPs were detected²⁴. In the present study, we investigated the expression of HSPs under hypoxic conditions of blood flow stasis. We immunohistochemically examined intrathrombotic appearance of HSP27 and HSP70 and discussed the possibility of their application to thrombus age estimation in forensic practices.

Results

Intrathrombotic HSP27 and HSP70 expressions after the inferior vena cava (IVC) ligation

The intrathrombotic gene expressions of *Hspb1* (*Hsp27*) and *Hspa1a* (*Hsp70*) were observed on day 3, then increased and was highest on day 10, and then decreased (Fig. 1a and b). The trend of increase or decrease in the expression of both genes was consistent with that of the number of positive cells determined from immunohistochemistry (Fig. 1c).

Intrathrombotic distributions of HSPs and macrophages

Fluorescence double staining analysis showed that the intrathrombotic localizations of HSP27⁺ or HSP70⁺ cells and F4/80⁺ macrophages were consistent (Fig. 2a and b). In addition, most F4/80⁺ cells expressed CD11b (another macrophage maker), and CD11b⁺ cells expressed both HSP27 and HSP70 (Fig. 2c–e). In contrast, MPO⁺ neutrophils, α -SMA⁺ fibroblasts, and CD31⁺ endothelial cells did not express HSPs (Fig. 3). These results suggested that macrophages were the main producers of both HSP27 and HSP70 in the thrombi.

Intrathrombotic appearance of HSP27⁺ or HSP70⁺ cells

In the sub-acute and chronic phase thrombi, the HSP27⁺ and HSP70⁺ cells were detected (Fig. 1c and Table 1). Until day 10, when the inflammatory response is dominant in thrombus formation²⁵, the number of HSP27⁺ cells exceeded the number of HSP70⁺ cells (Fig. 4). The HSP27⁺ cells were more abundant than HSP70⁺ cells until the thrombus entered the chronic phase, and by day 10, HSP27⁺ cells were significantly more numerous than HSP70⁺ cells, but by day 14, both HSP27 and HSP70 were almost the same. These results suggest that the kinetics of HSP27 and HSP70 expression in thrombus can be a useful index for determining the degree of obsolescence of thrombus even in autopsy cases.

Both HSP27 and HSP70 inhibitors reduced thrombi size in mice

In another experiment, mice were treated with HSP27 or HSP70 inhibitors to explore the role of HSPs. Five days after IVC ligation, mice treated with pharmacological inhibitors of HSP27 or HSP70 developed smaller thrombi compared to PBS-treated control mice (Fig. 5a,b,d,e). Furthermore, blood flow was increased in mice treated with inhibitors compared to control mice (Fig. 5c and f). These observations suggest that HSP27 and HSP70 may play an important role in the pathogenesis of thrombosis.

Estimation of thrombus age using human samples

In the next step, thrombus samples collected from human were analyzed histopathologically and immunohistochemically to estimate thrombus age (No. 1 to 7 in Fig. 6 and Table 2). As an example, No.1, the thrombus showed that the collagen content area was approximately 45% and number of hemosiderin-positive cells was 33 (Fig. 6a and Table 2). In addition, the ratio of MPO-positive neutrophils to CD68-positive macrophages (N/M ratio) referred to 0.9 (Fig. 6a and Table 2). Moreover, the number of HSP70-positive cells was markedly lower than that of HSP27-positive cells. (Fig. 6a and Table 2) Taken together, these observations suggest that the human thrombus No. 1 may be 7–10 days old based on our findings^{25,26}. The thrombi from No. 2 to 7 were analyzed in the same way and the thrombus age was estimated (Fig. 6b–g and Table 2).

Discussion

The expression of HSPs in the lungs, myocardium, and kidneys under heat stress was clear, and their expression was a useful indicator for estimating the cause of death and time since death^{22–24}. To elucidate the types of stresses under which HSPs are expressed, we confirmed their expression in experimental thrombi. HSPs were identified not only in experimental thrombi but also in thrombi found postmortem, suggesting that the relationship between thrombi and HSPs is also an important factor. In fact, the degree of thrombus patency was closely related to HSP expression.

In this study, we performed immunohistochemical search for heat shock proteins, especially HSP27 and HSP70. HSP27 is ubiquitously present in both the cytoplasm and nucleus, and its expression level increases upon exposure to heat shock and various stress conditions. The major roles of HSP27 include regulation of protein folding by chaperone function, protein degradation, maintenance of the cytoskeleton, regulation of the

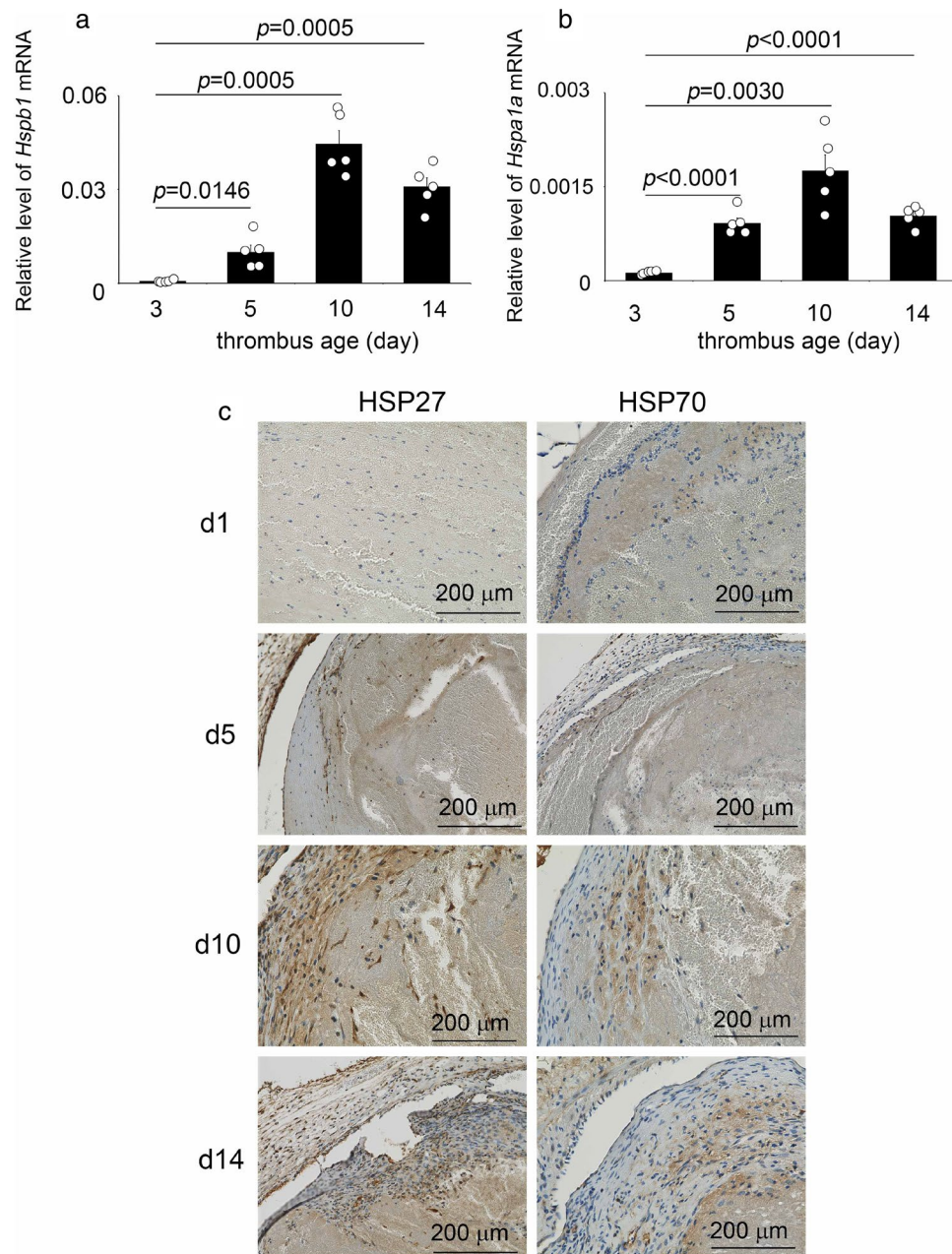


Figure 1. Intrathrombotic expressions of HSP27 and HSP70 in mice. **(a and b)** Intrathrombotic gene expressions of *Hspa1a* and *Hspb1* were examined by real-time RT-PCR in mice after inferior vena cava (IVC) ligation. *Hspb1*: murine HSP27 gene; *Hspa1a*: murine HSP70 gene. $n = 5$ in each group. **(c)** Immunohistochemical analysis of HSP27 and HSP70 in mouse thrombi. Representative results were shown ($n = 5$).

cell cycle, immune response, promotion of cancer, induction of resistance to anticancer drugs, aging, biomarkers of disease, exacerbation of neurodegenerative diseases, development, and differentiation^{6–9,27–36}. HSP70s are abundant in cancer cells and have been shown to suppress multiple apoptotic pathways, regulate necrosis, evade cellular senescence programs, interfere with tumor immunity, promote angiogenesis, and even affect tumor metastasis^{6,8,30}.

Recently, Thienel et al. reported that distinct antithrombotic patterns were detected in the platelets of hibernating brown bears. Among these, HSP47, which is an essential intracellular chaperone molecule for facilitating collagen production within cells that secrete collagen, showed the most notable decrease. Lowering or eliminating HSP47 led to the inhibition of immune cell activation and the formation of neutrophil extracellular traps, contributing to the prevention of blood clotting in bears, patients with spinal cord injuries, and mice³⁷. In addition, HSP47 was reported to be present on the platelet surface, where it interacts with collagen, stabilizes platelet adhesion, and increases collagen-mediated signaling, thus promoting thrombus formation and

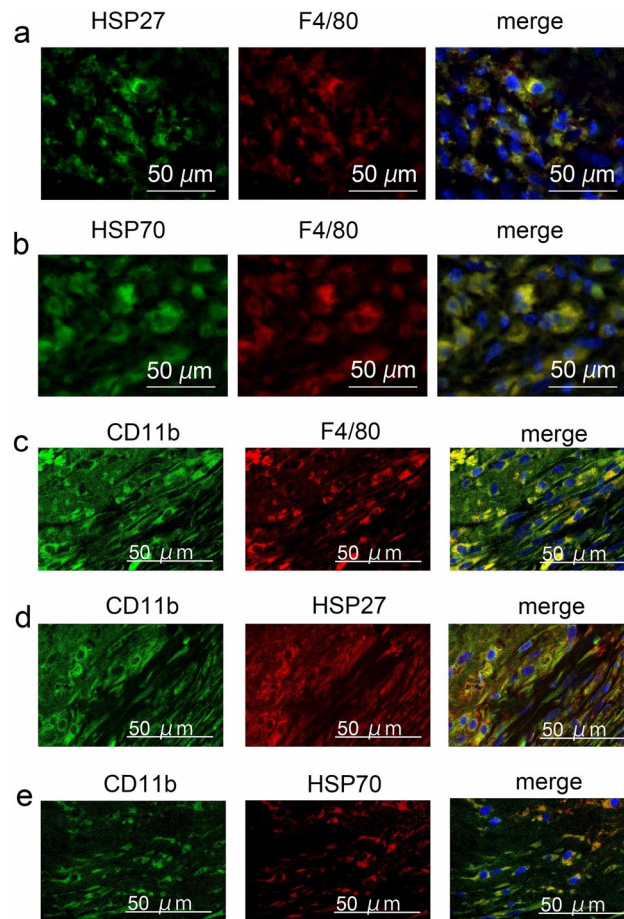


Figure 2. Double-color immunofluorescence analysis of HSPs and F4/80 or CD11b in the 14-days-thrombi. (a) HSP27 (green), F4/80 (red) and DAPI (blue); (b) HSP70 (green), F4/80 (red) and DAPI (blue); (c) CD11b (green), F4/80 (red) and DAPI (blue); (d) CD11b (green), HSP27 (red) and DAPI (blue); (e) CD11b (green), HSP70 (red) and DAPI (blue).

hemostasis³⁸. On the other hand, ex vivo, pharmacological inhibition of Hsp70 in human whole blood prevented the formation of platelet aggregates on collagen under shear³⁹. In fact, we found that both HSP70 and HSP27 inhibitors showed reduced thrombi mass in mice. These findings of these HSPs could serve as the foundation for a new protective mechanism against the development of thrombus formation.

We found a relationship between the degree of thrombosis and the expression of HSPs in a DVT model. Although few positive cells and gene expressions were observed until the third day of thrombus formation, both HSP27 and HSP70 increased from the 5-day to the 10-day, suggesting that the stress of IVC ligation and the subsequent initiation of blood coagulation induced these HSPs expressions. The intrathrombotic HSPs were mainly expressed on F4/80⁺ macrophages to promote thrombolysis, and were involved in the formation of intrathrombotic neovessels. Although the expression period of HSPs was short, ranging from 5 to 14 days, HSP27 was expressed in large numbers and clearly, especially on 10-day, and may be a useful indicator to determine the age of thrombosis.

Taken together, our observations implied that both HSP27 and HSP70 might be a molecular target for thrombus therapy from the aspects of clinical relevance. Moreover, the detection of intrathrombotic HSP27 and HSP70 could provide useful information for the estimation of thrombus ages with potential applications in forensics. Collectively, our findings support the interdisciplinary, multifaceted nature of both HSP27 and HSP70.

Materials and methods

Stasis-induced deep vein thrombus model

Specific pathogen-free 8- to 10-week-old male BALB/c mice were purchased from SLC (Shizuoka, Japan). Intravenous thrombus was induced as described previously^{11–14}. Under the deep anesthesia by isoflurane inhalation (FUJIFILM Wako Pure Chemical Corporation, Osaka, Japan), an incision was made on the abdominal wall, and the inferior vena cava (IVC) was exposed and ligated. At the indicated time intervals, mice were euthanized by the inhalation of over-dose isoflurane, and thrombus samples were obtained. We used 5 mice at each time point. In another series, BALB/c mice were treated intraperitoneally HSP27 inhibitor (50 μg/mouse/day; HY-124653, MedChemExpress, Monmouth Junction, NJ) or HSP70 inhibitor (0.1 mM/mouse/day; A18734,

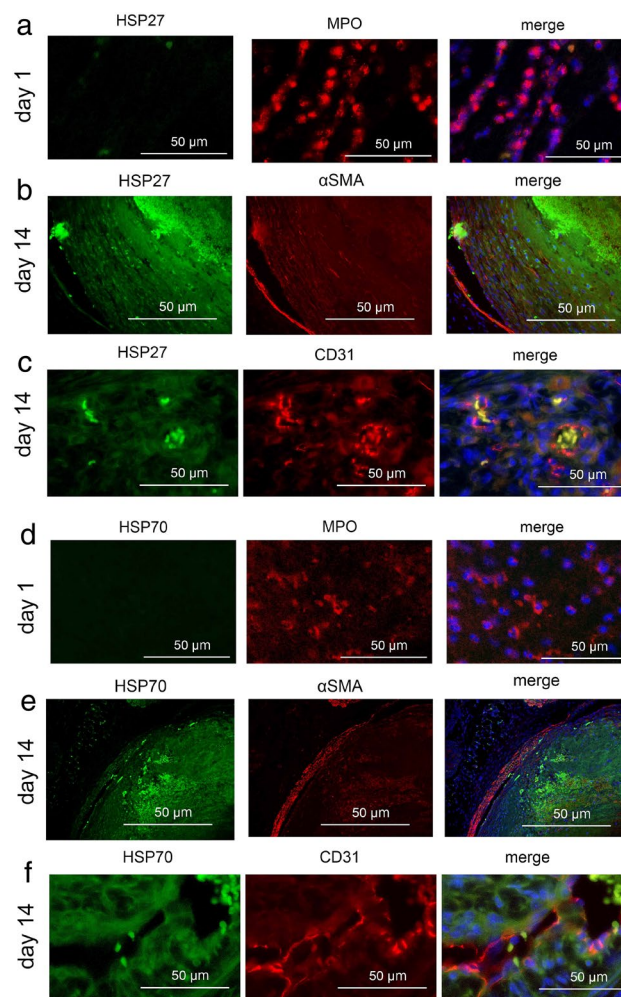


Figure 3. Double-color immunofluorescence analysis of HSPs and MPO, α -SMA, or CD31 in the thrombi at the indicated time points. **(a)** HSP27 (green), MPO (red) and DAPI (blue); **(b)** HSP27 (green), α -SMA (red) and DAPI (blue); **(c)** HSP27 (green), CD31 (red) and DAPI (blue); **(d)** HSP70 (green), MPO (red) and DAPI (blue); **(e)** HSP70 (green), α -SMA (red) and DAPI (blue); **(f)** HSP70 (green), CD31 (red) and DAPI (blue).

Thrombus age (day)	HSP27 ⁺ cells Mean \pm SEM (range)	HSP70 ⁺ cells Mean \pm SEM (range)
1	0	1.00 \pm 0.37 (0–2)
3	0.60 \pm 0.00 (0–3)	1.20 \pm 0.56 (0–3)
5	7.80 \pm 1.48 (0–11)	5.20 \pm 1.95 (2–11)
7	10.00 \pm 2.22 (4–15)	6.00 \pm 2.59 (0–15)
10	23.00 \pm 1.80 (18–27)	13.20 \pm 3.62 (3–21)
14	14.20 \pm 0.73 (12–16)	13.00 \pm 0.99 (8–17)
21	5.00 \pm 0.82 (3–7)	7.00 \pm 1.10 (5–10)

Table 1. Mean intrathrombotic HSP27⁺ cells and HSP70⁺ cell numbers (n = 5).

Adooq BioScience, Irvine, CA), or PBS as controls at one day before the IVC ligation and at 1 and 3 days after the IVC ligation. At day 5 after the IVC ligation, intravenous thrombi were harvested for the determination of the weights and blood flow. Five to six mice were used per group. All animal experiments were approved by the Committee on Animal Care and Use of Wakayama Medical University.

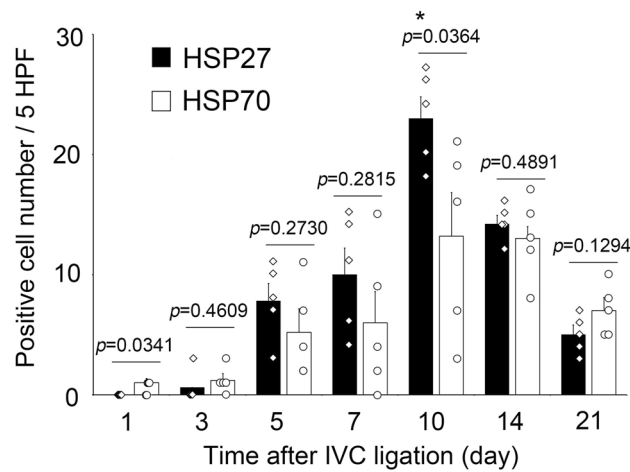


Figure 4. Changes in intrathrombotic HSP27⁺ cell and HSP70⁺ cell numbers after IVC ligation. Both positive cell number of HSP27 and HSP70 showed maximum values on day 10, but HSP27 was significantly abundant than HSP70. $n = 5$ in each group.

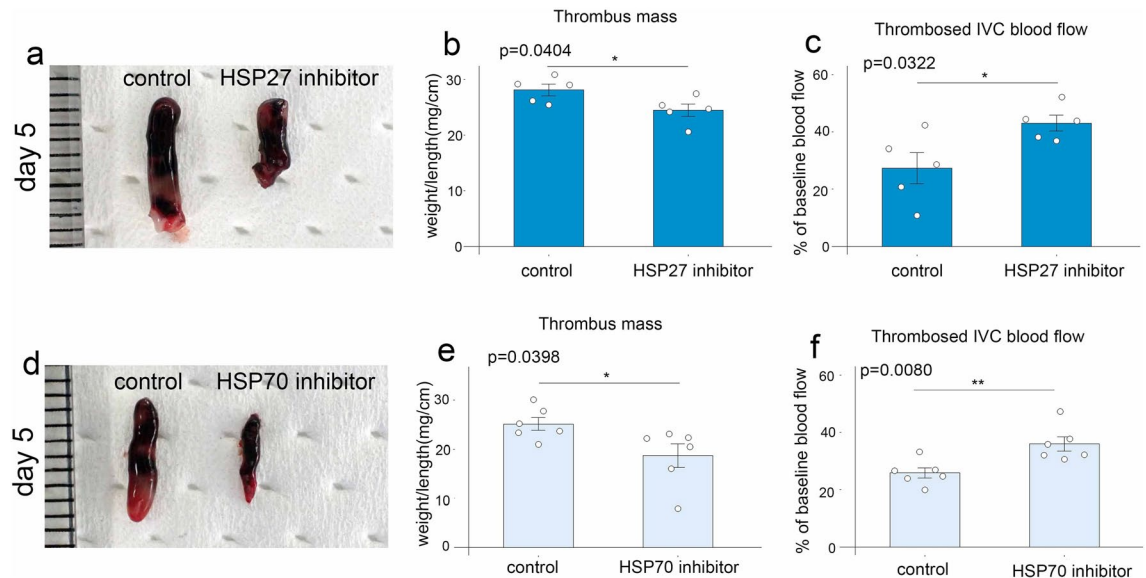


Figure 5. The effects of HSP27 and HSP70 inhibitor in murine thrombosis. (a) Macroscopic appearance of venous thrombi obtained from mice treated with HSP27 inhibitor or PBS as controls. Representative results from five independent animals are shown. Thrombus mass (b) and thrombosed blood flow (c) were measured at 5 days after IVC ligation. (d) Macroscopic appearance of venous thrombi obtained from mice treated with HSP70 inhibitor or PBS as controls. Representative results from six independent animals are shown. Thrombus mass (e) and thrombosed blood flow (f) were measured at 5 days after IVC ligation. All values represent the mean \pm SEM ($n = 5$ –6 animals). ** $p < 0.01$, * $p < 0.05$ vs. control.

Human deep vein thrombus samples

A total of 7 human thrombus samples were collected from forensic autopsy cases with a postmortem interval (PMI) of less than 72 h. The individual ages ranged from 33 to 90 years (mean age, 65.1 years). Samples were subjected to subsequent analyses.

Histopathological analysis and immunohistochemistry

The thrombus samples were fixed in 4% formaldehyde buffered with PBS (pH 7.2) for 24 h, and 4- μ m-thick paraffin-embedded sections were made^{11,40}. For mice thrombi, immunostaining of HSP27 and HSP70 were performed by Ventana Discovery XT (Ventana Medical Systems, Inc., AZ, USA) using mouse anti-HSP27 monoclonal antibodies (mAbs) (sc-13132, Santa Cruz Biotechnology, Inc., Santa Cruz CA, USA), mouse anti-HSP70 mAb (sc-32239, Santa Cruz Biotechnology, Inc., Santa Cruz CA, USA). On the other hand, for human thrombi, the sections were stained with Hematoxylin and eosin (HE), Masson's Trichrome (MT), and Berlin

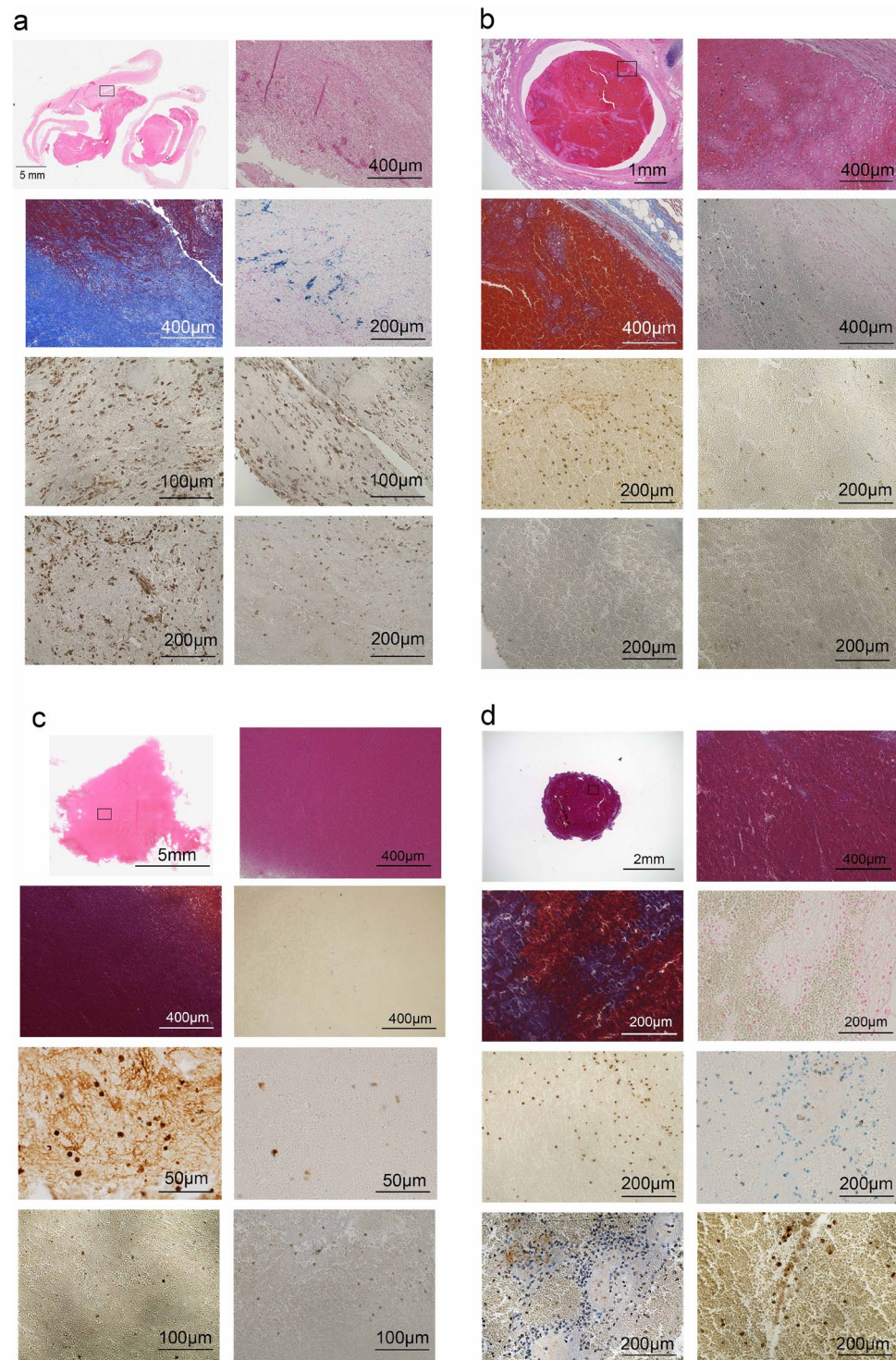


Figure 6. Histopathological and immunohistochemical images of human thrombi. As show in Table 2, case 1 (a); case 2 (b); case 3 (c); case 4 (d); case 5 (e); case 6 (f); and case 7 (g). (h) Staining indication panels in (a) to (c).

blue after deparaffinization^{12–14,26}. As described previously, immunostaining of HSP27, HSP70, myeloperoxidase (MPO), and CD68 were performed by Ventana Discovery XT using mouse anti-HSP27 mAb (sc-13132, Santa Cruz Biotechnology), mouse anti-HSP70 mAb (sc-32239, Santa Cruz Biotechnology), rabbit anti-MPO pAbs (RB-373-A, Lab Vision/Neo Markers, Fremont, CA), and mouse anti-CD68 mAb (clone PG-M1, M0876, DAKO, Glostrup, Denmark)^{11,13,14}. After incubating the specimens with HRP-conjugated anti-mouse multimer (518-102128, OmniMap HRP Multimer, Roche Diagnostics K.K., Tokyo, Japan), immune complexes were

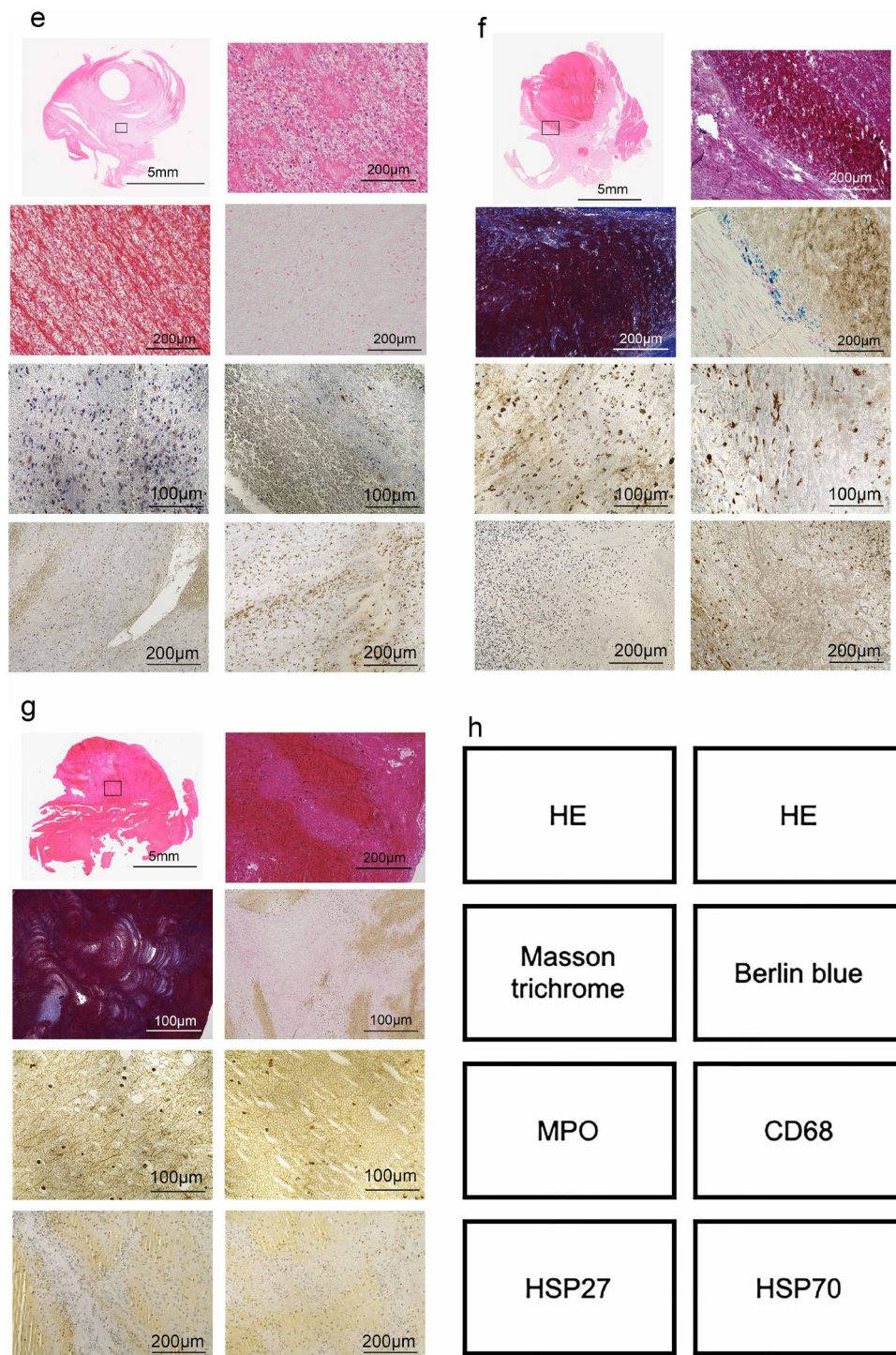


Figure 6. (continued)

visualized using Chromomax kit DAB (518-100803, Roche Diagnostics K.K.) according to the manufacturer's instructions. The number of cells positive for HSP27⁺ and HSP70⁺ in mice and human thrombi were evaluated semi-quantitatively as described previously^{11,14,41}. Immunopositive cells were enumerated in five high-power fields (hpf, ×1000) within the thrombus, the total numbers in the five fields were combined. All measurements were performed by two examiners without prior knowledge.

Double-color immunofluorescence analysis

Double-color immunofluorescence analysis of HSP27 and F4/80 (MCA497, Bio-Rad Laboratories, Hercules, CA), CD11b (rabbit anti-CD11b mAb, ab133357, clone EPR1344, Abcam, Cambridge, UK), MPO (rabbit anti-MPO pAb, RB-373-A, Lab Vision/Neo Markers), α-SMA (mouse anti-α-SMA mAb, ab7817, clone 1A4,

Case	Collagen content area (%) collagen area/ thrombus area (pixels)	Hemosiderin-positive cell number	N/M ratio	HSP27 ⁺ cells	HSP70 ⁺ cells	Estimated thrombus age (day)
No. 1	85.1/186.7 = 45.6	33	52/56 = 0.9	27	17	7–10
No. 2	0.3/15.7 = 1.9	0	63/13 = 4.8	5	9	1–3
No. 3	0.6/102.5 = 0.6	3	81/15 = 5.4	3	2	1–3
No. 4	0.2/5.4 = 3.7	0	97/35 = 2.8	10	12	3–5
No. 5	0.7/86.7 = 0.8	0	47/6 = 7.8	7	13	1–3
No. 6	4.2/41.8 = 10.0	12	44/17 = 2.6	6	11	3–5
No. 7	4.4/195.4 = 2.2	0	31/8 = 3.9	6	3	1–3

Table 2. Determination of human thrombus age.

Abcam), or CD31 (rat anti-CD31 mAb, clone MEC 13.3, BD Biosciences, Franklin Lakes, NJ), and HSP70 and F4/80 or CD11b were performed by Ventana Discovery XT¹³. Deparaffinized-sections were incubated in a combination of mouse anti-HSP27 mAb and rat anti-F4/80 mAb or anti-HSP70 mAb and rat anti-F4/80 mAb. After incubation with FITC-labelled (3 µg/ml, Jackson Immunoresearch Laboratories, West Grove, PA) and Cy3-labelled secondary pAbs (0.75 µg/ml, Jackson Immunoresearch Laboratories), the sections were observed by fluorescence microscopy^{16,18}. Each section was enclosed using mounting medium for fluorescence with DAPI (H-1200Vectashield, Vector).

Morphometrical analysis of collagen deposition, histopathological and immunohistochemical staining of human thrombi

We analyzed collagen accumulation, hemosiderin-positive cell counts, and neutrophil/macrophage ratios in seven autopsy thrombi. The most critical event for the formation of thrombi is the rise in collagen content within the thrombus. We have previously reported that measurement of collagen accumulation in mouse thrombus is useful for estimating thrombus age²⁶. Therefore, intrathrombotic collagen deposition was semi-quantitated as the blue area in MT-stained sections. The area of collagen deposition in the thrombus was evaluated by Image J analysis software Ver. 1.38w (National Institute of Health, USA), and expressed as the percentage of the whole thrombus area. For semiquantitative evaluation of Berlin blue staining sections, morphometrical analysis was performed, as described previously²⁶. Briefly, in each section, five microscopic fields (two central and three peripheral fields) were randomly selected (magnification 1000×), and the number of hemosiderin-positive cells within the thrombi were counted and summed from the five microscopic fields. Moreover, in each section, five microscopic fields were randomly selected (1000×), and the number of MPO-positive neutrophils and CD68-positive macrophages within the thrombi were counted and summed from the five microscopic fields²⁵. Thereafter the ratios of neutrophils to macrophages (N/M ratios) were calculated.

Extraction of total RNAs and real-time RT-PCR

Real-time RT-PCR was performed as described previously^{12–14}. Briefly, total RNA was extracted from thrombus tissue samples using ISOGEN (Nippon Gene, Toyama, Japan) according to the manufacturer's instructions, and 1 µg of total RNAs were reverse-transcribed into cDNA at 42 °C for 1 h in 20 µl reaction mixture containing mouse Moloney leukemia virus reverse transcriptase (PrimeScript, TAKARA BIO, Shiga, Japan) with random 6 primers (TAKARA BIO). Thereafter, generated cDNA was subjected to real-time PCR analysis using TB Green Premix Ex Taq II (TAKARA BIO) with the sets of specific primers (Table 3). Relative quantity of the target gene expression to β-actin gene was measured by comparative Ct method.

Statistical analysis

All data are presented as the mean ± SEM. To compare the values between two groups, Student *t* test was performed. All statistical analyses were performed using Microsoft Excel. *p* < 0.05 was accepted as significant. For human thrombus samples, all data are presented as the mean ± SEM. Statistical significance was evaluated using Mann–Whitney's *U*-test. *P* < 0.05 was accepted as significant.

Transcript	Sequences
<i>Hspb1</i>	(F) 5'-TCCCTGGACGTCAACCACTTC-3'
	(R) 5'-AGAGATGTAGCCATGTCGTCCTG-3'
<i>Hspa1a</i>	(F) 5'-GTGGTTGCACCTGACTTGTTC-3'
	(R) 5'-GACCCGAGTTCAGGATGTTG-3'
β-actin	(F) 5'-CATCCGTAAGACCTCTATGCCAAC-3'
	(R) 5'-ATGGAGCCACCGATCCACA-3'

Table 3. Sequences of the primers used for real-time RT-PCR. *F* forward primer, *R* reverse primer.

Ethical approval

All animal experiments were approved by the Committee on Animal Care and Use at Wakayama Medical University (No. 1082) and all methods were performed in accordance with relevant regulations and guidelines including the ARRIVE guideline. This study was approved by the Research Ethics Committee of Wakayama Medical University (No. 3314) regarding the use of human samples. All the procedures were performed in accordance with the Declaration of Helsinki Principles. Moreover, this study was conducted using autopsy records from the past, and we could not obtain informed consent from the bereaved family for the use of these records. Therefore, we conducted this study in accordance with the "Ethical Guidelines for Medical Research Involving Human Subjects (enacted by the Ministry of Health, Labor, and Welfare in Japan), section 12–1 (2) (a) (c)." This was a de-identified study using archived tissue obtained from judicial autopsy cases, and the information on the implementation of the study was posted on our website (<https://www.wakayama-med.ac.jp/dept/igakubu/160420/index.html>). The review board of the Research Ethics Committee of Wakayama Medical University waived the need for written informed consent from the relatives of the individuals studied in accordance with the national legislation and the institutional requirements.

Data availability

The authors declare that all data are available in the article file or available from the corresponding author, Toshikazu Kondo, upon reasonable request.

Received: 1 December 2022; Accepted: 2 December 2023

Published online: 16 December 2023

References

- Choi, S.-H. *et al.* MMP9 processing of HSPB1 regulates tumor progression. *PLoS ONE* <https://doi.org/10.1371/journal.pone.0085509> (2014).
- Voss, O. H. *et al.* Binding of caspase-3 prodomain to heat shock protein 27 regulates monocyte apoptosis by inhibiting caspase-3 proteolytic activation. *J. Biol. Chem.* **282**(34), 25088–25099. <https://doi.org/10.1074/jbc.M701740200> (2007).
- Concannon, C. G., Orrenius, S. & Samali, A. Hsp27 inhibits cytochrome c-mediated caspase activation by sequestering both pro-caspase-3 and cytochrome c. *Gene Expr.* **9**(4–5), 195–201. <https://doi.org/10.3727/00000001783992605> (2001).
- Jana, N. R., Tanaka, M., Wang, G. H. & Nukina, N. Polyglutamine length-dependent interaction of Hsp40 and Hsp70 family chaperones with truncated N-terminal huntingtin: Their role in suppression of aggregation and cellular toxicity. *Hum. Mol. Genet.* **9**, 2009–2018. <https://doi.org/10.1093/hmg/9.13.2009> (2000).
- Singh, M. K., Sharma, B. & Tiwari, P. K. The small heat shock protein Hsp27: Present understanding and future prospects. *J. Therm. Biol.* **69**, 149–154. <https://doi.org/10.1016/j.jtherbio.2017.06.004> (2017).
- Kumar, S. Jr. *et al.* Targeting Hsp70: A possible therapy for cancer. *Cancer Lett.* **374**, 156–166. <https://doi.org/10.1016/j.canlet.2016.01.056> (2016).
- Borges, T. J. *et al.* The anti-inflammatory mechanisms of Hsp70. *Front. Immunol.* <https://doi.org/10.3389/fimmu.2012.00095> (2012).
- Albakova, Z., Armeev, G. A., Kanevskiy, L. M., Kovalenko, E. I. & Sapozhnikov, A. M. HSP70 multi-functionality in cancer. *Cells* <https://doi.org/10.3390/cells9030587> (2020).
- Chebotaeva, N., Bobkova, I. & Shilov, E. Heat shock proteins and kidney disease: Perspectives of HSP therapy. *Cell Stress Chaperones* **22**, 319–343. <https://doi.org/10.1007/s12192-017-0790-0> (2017).
- Nosaka, M., Ishida, Y., Kimura, A. & Kondo, T. Immunohistochemical detection of MMP-2 and MMP-9 in a stasis-induced deep vein thrombosis model and its application to thrombus age estimation. *Int. J. Legal Med.* **124**, 439–444. <https://doi.org/10.1007/s00414-010-0484-y> (2010).
- Nosaka, M. *et al.* The application of autophagy to thrombus age estimation in murine deep vein thrombosis model. *Int. J. Legal Med.* **134**, 1061–1066. <https://doi.org/10.1007/s00414-019-02168-0> (2020).
- Nosaka, M. *et al.* Contribution of the TNF- α (tumor necrosis factor- α)-TNF-Rp55 (tumor necrosis factor receptor p55) axis in the resolution of venous thrombus. *Arterioscler. Thromb. Vasc. Biol.* **38**, 2638–2650. <https://doi.org/10.1161/ATVBAHA.118.311194> (2018).
- Nosaka, M. *et al.* Crucial involvement of IL-6 in thrombus resolution in mice via macrophage recruitment and the induction of proteolytic enzymes. *Front. Immunol.* **10**, 3150. <https://doi.org/10.3389/fimmu.2019.03150> (2019).
- Nosaka, M. *et al.* Absence of IFN- γ accelerates thrombus resolution through enhanced MMP-9 and VEGF expression in mice. *J. Clin. Investig.* **121**, 2911–2920. <https://doi.org/10.1172/JCI40782> (2011).
- Ishida, Y., Kimura, A., Takayasu, T., Eisenmenger, W. & Kondo, T. Expression of oxygen-regulated protein 150 (ORP150) in skin wound healing and its application for wound age determination. *Int. J. Legal Med.* **122**, 409–414. <https://doi.org/10.1007/s00414-008-0255-1> (2008).
- Ishida, Y., Kimura, A., Takayasu, T., Eisenmenger, W. & Kondo, T. Detection of fibrocytes in human skin wounds and its application for wound age determination. *Int. J. Legal Med.* **123**, 299–304. <https://doi.org/10.1007/s00414-009-0320-4> (2009).
- Ishida, Y. *et al.* Immunohistochemical analysis on cyclooxygenase-2 for wound age determination. *Int. J. Legal Med.* **126**, 435–440. <https://doi.org/10.1007/s00414-012-0685-7> (2012).
- Ishida, Y. *et al.* Detection of endothelial progenitor cells in human skin wounds and its application for wound age determination. *Int. J. Legal Med.* **129**, 1049–1054. <https://doi.org/10.1007/s00414-015-1181-7> (2015).
- Ishida, Y. *et al.* Immunohistochemical analysis on MMP-2 and MMP-9 for wound age determination. *Int. J. Legal Med.* **129**, 1043–1048. <https://doi.org/10.1007/s00414-015-1167-5> (2015).
- Kimura, A. *et al.* Autophagy in skin wounds: A novel marker for vital reactions. *Int. J. Legal Med.* **129**, 537–541. <https://doi.org/10.1007/s00414-015-1168-4> (2015).
- Kuninaka, Y. *et al.* Forensic pathological study on temporal appearance of dendritic cells in skin wounds. *Int. J. Legal Med.* **134**, 597–601. <https://doi.org/10.1007/s00414-019-02185-z> (2020).
- Doberentz, E., Gennep, L., Wagner, R. & Madea, B. Expression times for hsp27 and hsp70 as an indicator of thermal stress during death due to fire. *Int. J. Legal Med.* **131**, 1707–1718. <https://doi.org/10.1007/s00414-017-1566-x> (2017).
- Doberentz, E., Gennep, L., Böker, D., Lignitz, E. & Madea, B. Expression of heat shock proteins (hsp) 27 and 70 in various organ systems in cases of death due to fire. *Int. J. Legal Med.* **128**, 967–978. <https://doi.org/10.1007/s00414-014-0994-0> (2014).
- Prangenberg, J., Doberentz, E., Mawick, A. & Madea, B. Mini review: The forensic value of heat shock proteins. *Front. Med.* **8**, 800100. <https://doi.org/10.3389/fmed.2021.800100> (2021).

25. Nosaka, M., Ishida, Y., Kimura, A. & Kondo, T. Time-dependent appearance of intrathrombus neutrophils and macrophages in a stasis-induced deep vein thrombosis model and its application to thrombus age determination. *Int. J. Legal Med.* **123**(3), 235–240. <https://doi.org/10.1007/s00414-009-0324-0> (2009).
26. Nosaka, M., Ishida, Y., Kimura, A. & Kondo, T. Time-dependent organic changes of intravenous thrombi in stasis-induced deep vein thrombosis model and its application to thrombus age determination. *Forensic Sci. Int.* **195**(1–3), 143–147. <https://doi.org/10.1016/j.forsciint.2009.12.008> (2010).
27. Calderwood, S. K. & Gong, J. Heat Shock Proteins Promote Cancer: It's a protection racket. *Trends Biochem. Sci.* **41**, 311–323. <https://doi.org/10.1016/j.tibs.2016.01.003> (2016).
28. Wrońska, A. K. & Boguś, M. I. Heat shock proteins (HSP 90, 70, 60, and 27) in *Galleria mellonella* (Lepidoptera) hemolymph are affected by infection with *Conidiobolus coronatus* (Entomophthorales). *Trends Biochem. Sci.* <https://doi.org/10.1016/j.tibs.2016.01.003> (2020).
29. Bårdsen, K. *et al.* Heat shock proteins and chronic fatigue in primary Sjögren's syndrome. *Innate Immun.* **22**, 162–167. <https://doi.org/10.1177/1753425916633236> (2016).
30. Jagdish, N. *et al.* Heat shock protein 70–2 (HSP70-2) is a novel therapeutic target for colorectal cancer and is associated with tumor growth. *BMC Cancer* **16**, 561. <https://doi.org/10.1186/s12885-016-2592-7> (2016).
31. Martine, P. & Rébé, C. Heat shock proteins and inflammasomes. *Int. J. Mol. Sci.* <https://doi.org/10.3390/ijms20184508> (2019).
32. Chebotareva, N. *et al.* Heat shock protein 70 and anti-heat shock protein 70 antibodies in patients with chronic glomerulonephritis. *Cell Stress Chaperones* **23**, 1229–1235. <https://doi.org/10.1007/s12192-018-0928-8> (2018).
33. Yombo, D. J. K., Mentink-Kane, M. M., Wilson, M. S., Wynn, T. A. & Madala, S. K. Heat shock protein 70 is a positive regulator of airway inflammation and goblet cell hyperplasia in a mouse model of allergic airway inflammation. *J. Biol. Chem.* **294**, 15082–15094. <https://doi.org/10.1074/jbc.RA119.009145> (2019).
34. Choi, S.-K., Kam, H., Kim, K.-Y., Park, S. I. & Lee, Y.-S. Targeting heat shock protein 27 in cancer: A druggable target for cancer treatment?. *Cancers* <https://doi.org/10.3390/cancers11081195> (2019).
35. Oya-Ito, T., Takagi, T., Shima, K. & Naito, Y. Expression and post-translational modification of heat shock protein 27 (HSP27) in cancer. *Therm. Med.* **36**, 1–24. <https://doi.org/10.3191/thermalmed.36.1> (2020).
36. Ozawa, K. *et al.* Expression of the oxygen-regulated protein ORP150 accelerates wound healing by modulating intracellular VEGF transport. *J. Clin. Investig.* **108**, 41–50. <https://doi.org/10.3191/thermalmed.36.1> (2001).
37. Thienel, M. *et al.* Immobility-associated thromboprotection is conserved across mammalian species from bear to human. *Science*. **380**(6641), 178–187. <https://doi.org/10.1126/science.abo5044> (2023).
38. Sasikumar, P. *et al.* The chaperone protein HSP47: A platelet collagen binding protein that contributes to thrombosis and hemostasis. *J. Thromb. Haemost.* **16**(5), 946–959. <https://doi.org/10.1111/jth.13998> (2018).
39. Dieudé, M. *et al.* Autoantibodies to heat shock protein 60 promote thrombus formation in a murine model of arterial thrombosis. *J. Thromb. Haemost.* **7**(4), 710–719. <https://doi.org/10.1111/j.1538-7836.2009.03305.x> (2009).
40. Barranco, R., Castiglioni, C., Ventura, F. & Fracasso, T. Immunohistochemical expression of P-selectin, SP-A, HSP70, aquaporin 5, and fibronectin in saltwater drowning and freshwater drowning. *Int. J. Legal Med.* **133**, 1461–1467. <https://doi.org/10.1007/s00414-019-02105-1> (2019).
41. Cecchi, R. *et al.* Markers of mechanical asphyxia: Immunohistochemical study on autoptic lung tissues. *Int. J. Legal Med.* **128**, 117–125. <https://doi.org/10.1007/s00414-013-0876-x> (2014).

Acknowledgements

We thank Ms. Mariko Kawaguchi for her excellent assistance in the preparation of this manuscript. This study was financially supported in part by Grants-in-Aids for Scientific Research (C, 22K10615, M.N.) from the Japan Society for the Promotion of Science (JSPS).

Author contributions

M.N. and T.K. formulated the hypothesis and designed the project; M.N. performed the main experiments; Y.I., Y.K., A.I., and A.K. provided technical assistance and discussion; A.T., E.S., Y.H. and H.Y. helped with some experimental procedures; F.F. and T.K. oversaw the experiments and provided the main funding for the project; M.N. Y.I. and T.K. participated in writing the manuscript.

Competing interests

The authors declare no competing interests.

Additional information

Correspondence and requests for materials should be addressed to T.K.

Reprints and permissions information is available at www.nature.com/reprints.

Publisher's note Springer Nature remains neutral with regard to jurisdictional claims in published maps and institutional affiliations.



Open Access This article is licensed under a Creative Commons Attribution 4.0 International License, which permits use, sharing, adaptation, distribution and reproduction in any medium or format, as long as you give appropriate credit to the original author(s) and the source, provide a link to the Creative Commons licence, and indicate if changes were made. The images or other third party material in this article are included in the article's Creative Commons licence, unless indicated otherwise in a credit line to the material. If material is not included in the article's Creative Commons licence and your intended use is not permitted by statutory regulation or exceeds the permitted use, you will need to obtain permission directly from the copyright holder. To view a copy of this licence, visit <http://creativecommons.org/licenses/by/4.0/>.

© The Author(s) 2023